

An Estimate of Mountain Drag during ALPEX for Comparison with Numerical Models

B. C. CARISSIMO

Atmospheric and Oceanic Sciences Program, Princeton University, Princeton, New Jersey

R. T. PIERREHUMBERT

Geophysical Fluid Dynamics Laboratory/NOAA, Princeton, New Jersey

H. L. PHAM

Centre de Recherche en Meteorologie Dynamique, Direction de la Meteorologie Nationale, Paris, France

(Manuscript received 28 August 1987, in final form 5 February 1988)

ABSTRACT

The pressure drag vector for a limited domain including the Alps is estimated for the ALPEX period of March and April 1982. All of the reported, three hourly, surface pressure data in the domain are used and maps of analyzed deviation surface pressure are obtained for the mountainous area. The very important drag values previously reported are confirmed and shown to occur when tight pressure gradients are localized above the steep orography. The peak values are found to be sensitive to the resolution of the analysis. A composite of the large drag variations occurring in relation to frontal passage and cyclogenesis is constructed. The diurnal cycle observed during periods of quiet synoptic activity is discussed. The observed drag compares favorably with the drag in the simulation of a case of cyclogenesis using a numerical model with comparable horizontal resolution.

1. Introduction

The determination of the mountain drag force on the atmosphere was among the main objectives of the Alpine Experiment (ALPEX, see Kuettner 1986). The experiment design included several sections across the topography, instrumented with microbarographs and accompanied, in some cases, by overhead flights by research aircraft.

Davies and Phillips (1985) have computed the local pressure drag across the Gotthard section using high frequency microbarograph surface pressure data. A notable feature in their time series is the strong drag (>5 Pa), reversing in 12 to 24 hours, which coincides with frontal passage and cyclogenesis over the Alps. They also found that the drag across the section is well correlated with the pressure difference between Stuttgart on the north side and Milano on the south side although the magnitude of the drag corresponding to a linear pressure gradient between these two stations is much too small. The large drag is due to the localization of the pressure drop within the Alpine inner region, giving rise to large pressure gradients that will certainly be underestimated by synoptic analyses.

A different method was used by Hafner and Smith

(1985) to compute the pressure drag vector caused by the entire Alpine range. Their method is based on a division of the Alps into subregions both in the horizontal and vertical directions. On each of these subregions Archimedes' law is applied, which gives the pressure force as the product of the topography volume and the locally constant pressure gradient. Strong variations, both in magnitude and direction, are found in relation with synoptic events in a manner consistent with the results of Davies and Phillips (1985).

The motivation for looking at this mountain drag and more generally for a better understanding of mountain effects came partly from the recognized deficiencies in representation of orography in numerical models. This aspect received growing attention recently, following the work of Wallace et al. (1983), which geographically links some of the systematic error in forecasts with the topography. As a result of this work, several semiempirical parameterizations of the effects of small scale, unresolved, topographic features have been proposed and used with some beneficial effects (Wallace et al. 1983; Boer et al. 1984; Palmer et al. 1986; Pierrehumbert 1987).

The results of ALPEX provide an observational basis against which these numerical models and parameterizations can be tested. In particular, these extremely strong values and rapid reversal of the drag represent a good test of adequate representation of topography in numerical simulations. They have been used, for

Corresponding author address: Dr. B. C. Carissimo, Direction des Etudes et Recherches, Electricité de France, 6 quai Watier 78401 Chatou Cedex, France.

example, by Tibaldi and Dell'Osso (1986) who showed that the model resolution is an important factor to reproduce the drag but also that the use of an envelope orography can lead to an overestimate of its magnitude.

In this paper we first present an evaluation of the drag vector due to the entire Alpine range, for the ALPEX period, using all the reported surface pressure data. The values of the drag we obtain are compared with those of Davies and Phillips (1985) who used only microbarograph data and those of Hafner and Smith (1985) who used only surface pressure data from a few carefully selected stations.

In section 2 we present the method of estimating the drag. Maps of analyzed pressure, obtained as an intermediate step, are discussed. The drag time series is presented in section 3 and a comparison with other studies follows. A composite of the strong drag events occurring in March is constructed in section 4. In section 5 we examine the influence of resolution upon the estimated drag and in section 6 we discuss the diurnal variations that are found in the time series. In section 7 we present a comparison of analyzed drag with the numerical simulation for a case of frontal passage and cyclogenesis. This is followed in section 8 by a summary of our results.

2. Principle of pressure drag evaluation

a. Method

The total force on an immersed body is composed of contributions from the tangential stress at the body surface and from the normal stress (Batchelor 1967). The contribution from the tangential stress, the frictional drag, will not be considered further here. In some applications, the total force due to the normal stress is further divided into different contributions such as the drag and lift in aerodynamics. Given the complex situations found in mountain meteorology we will not attempt to separate its different contributions, but rather consider it as one force. We will refer to its horizontal component as the pressure drag:

$$\mathbf{F} = \int_S p \mathbf{n} d\sigma, \quad (1a)$$

$$\mathbf{D} = -\mathbf{F}_H = - \int_S p \nabla h dx dy \quad (1b)$$

where

- \mathbf{F} total force acting on the mountain,
- \mathbf{D} drag acting on the atmosphere,
- p surface pressure,
- h mountain height,
- \mathbf{n} vector normal to the surface element $d\sigma$ and,
- S limited domain of integration.

Instead of following Hafner and Smith (1985) who transformed this integral in order to further simplify it by assuming a constant gradient, we directly compute

this integral from data. Therefore, an estimate of the fields of surface pressure and topography gradient is needed. We next describe how these quantities are obtained.

b. Surface pressure analysis

The surface pressure cannot be analyzed directly because its horizontal variation depends not only on the horizontal variation of the pressure field but also on the horizontal variation of the topography. A truly rigorous evaluation would require a three-dimensional analysis of the pressure field, in order to determine its value at the surface, which in turn would require the use of upper-air soundings which are clearly insufficient in number to adequately resolve the Alps (Richner 1986).

Instead, we follow a method inspired by Wahr and Oort (1984) which requires only the surface pressure data: $p[x, y, h(x, y), t]$ and which consists of removing the time and domain average pressure: $P[h(x, y)]$ at each station before doing the analysis on this resulting deviation pressure: $p'(x, y, t) = p - P$. This procedure is equivalent to an approximation, in the vertical interpolation, of the vertical pressure gradient ($\partial p / \partial z$) by the known average value (dP/dz). For simplicity in this study we have replaced the average pressure (P) by the standard atmosphere pressure.

The deviation pressure (p') is analyzed on a 0.5° grid in the domain $41^\circ - 49^\circ\text{N}$, $5^\circ - 16^\circ\text{E}$. An average of 180 station reports are used for the analysis in the domain considered (the exact number depends on the day and time of analysis).

In this method the reported pressure is first reduced, if necessary, to station pressure using a lapse rate of 6.5 K km^{-1} . Because all Alpine countries apply different reduction methods, this procedure might introduce errors. In general, however, the reported level is very close to the station level. For example, sea level pressure is reported only for low altitude stations whereas mountainous stations report surface pressure or geopotential height of the nearest standard level; therefore we expect the reductions errors to be minimal.

The limited domain of this study introduces difficulties compared with the global study by Wahr and Oort (1984). If the boundaries were all at the same level (as in a periodic domain) then the contribution from the average pressure (a function of z only) would be zero and the drag computed from the deviation (p') or surface pressure (p) would be the same. However, because, for example, the domain boundary is higher on the north side of the Alps than on the south side, the drag due to the average pressure is not zero. This drag, which physically corresponds to the horizontal component of the force resulting from the weight of the atmosphere on a domain that is not flat on average, is very large for our domain: the height difference between the northern and southern boundaries is typically 300 m for a domain size of 600 km, the average slope

is therefore 5×10^{-4} and gives a drag of approximately 50 Pa per unit area. This is a very large but constant value that depends solely on the geometrical characteristics of the domain.

Hafner and Smith (1985) avoided a similar problem by defining a sloping base for the Alps that was not taken into account for their volume computation, whereas Davies and Phillips (1985) carried out the integration for heights greater than 400 m.

In order to investigate some of the possible effects of data resolution on the drag values computed we have repeated the analysis, varying its resolution R by a change of the weighting function. Our fine analysis retains details on the scale of the average distance between surface data points (approximately $R = 50$ km). A coarser analysis which retains details on the scale of $R = 200$ km will be used to investigate the influence of a loss of resolution.

Figures 1a–c show an example of the analysis ($R = 50$ km) for the frontal passage of 4–5 March. The synoptic situation has been described, for example, by Hafner and Smith (1985). At 0000 UTC 4 March and at 0000 UTC 5 March the very strong pressure gradients can be seen above the topography and will give rise to very high drag values for these two times. Note also that these gradients have completely reversed in 24 h.

By contrast, the situation at 1200 UTC 4 March, during the drag reversal period, shows almost no pressure gradient across the topography and is therefore a case of weak drag. A similar sequence of events, with tight pressure gradients located near the crest of the Alps, is reproduced in all cases of frontal passage during the two months of ALPEx. They can be compared with other observations of orographically perturbed pressure (Smith 1982; Hoinka 1985; Steinacker 1981).

In Fig. 1d the NMC analysis of sea level pressure for 0000 UTC 5 March is shown for comparison (analysis provided by Bruce Wyman, GFDL, Princeton). Due to its low resolution (2.5°), compared to the present analysis (0.5°), it is unable to reproduce the tight gradients above the topography.

c. Topography

The topography we use is the high resolution Navy topography ($10' \times 10'$ grid), smoothed to the same resolution as the analyzed pressure fields. The smoothed gradients are obtained directly from the high resolution topography by convolution with the derivative of the filter function. Figure 2 shows an east–west cross section at 46°N for the topography at the two resolutions used. There is a sharp decrease in maximum height and magnitude of the gradients for the topography as the resolution is decreased.

3. Discussion of results

Using the surface pressure and topography gradients obtained as described above, the drag vector acting on

the atmosphere is computed according to Eq. (1) and for the Alpine region defined by the area of Fig. 1. The time series for the magnitude and direction of this drag vector are presented in Fig. 3 for the entire ALPEx Special Observing Period of March and April 1982. The convention used for the direction of the drag is the same as the one used for the wind direction. For example, a direction of 90° corresponds to an east to west drag force acting on the atmosphere. There is, however, no a priori simple relation between wind and drag directions. For example, in the case of south foehn on the Alps (southerly flow at low level, westerly flow at upper levels) the drag on the atmosphere is northerly.

Hafner and Smith (1985) and Davies and Phillips (1985) present detailed summaries for the weather events in March and April 1982 and show that there is a strong correlation between drag variations and the occurrence of synoptic events. The same correlation exists in the present study and we will only give a brief account of the sequence of weather events during the period to illustrate this fact. Three different periods, characterized by a persistence of the large scale weather pattern were identified.

- A first period (1–21 March), characterized by a baroclinically unstable westerly flow in which a series of cyclonic disturbances moved towards Europe. The associated frontal systems crossed the Alpine region from NW to SE and as many as six cases of lee cyclogenesis occurred during this period (2, 4–5, 11, 13, 18, 20–21 March).
- A second period (22 March–7 April) of transition with weaker and more variable wind that was not characterized by a persistent large scale weather pattern.
- A third period (8–30 April) characterized by a typical Euro–Atlantic blocking pattern with the blocking anticyclone located near Ireland. The flow in the proximity of the Alps came from a direction between northwest and east. The blocking anticyclone retreated slightly to the west on three occasions (8–9, 24–25, 29–30 April) and associated outbreaks of polar air reached the Mediterranean causing lee cyclogenesis in the last two cases only.

These periods in weather events have remarkable analogues in the time series of Fig. 3. The first period is characterized by large values and important variations of drag in close correspondence with the synoptic events mentioned above. A composite of these strong drag events will be presented in section 4. In the second period (the transition period) the drag is weaker than in the first period but variations in the direction are still important, although more gentle. The third period is characterized by weak drag values, except during the temporary disruption of the blocking pattern already mentioned. The drag direction is fairly constant throughout this third period.

Another notable feature of these drag time series is the diurnal oscillation in the magnitude, that can best be seen when the drag is weak in April, but that is

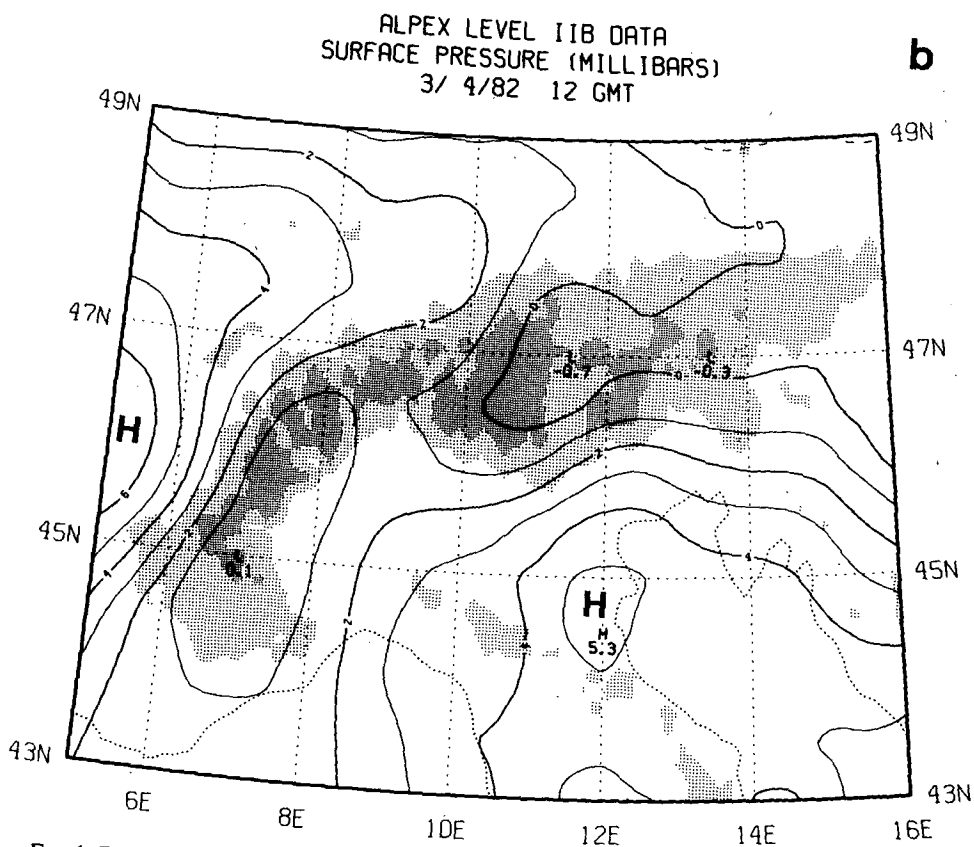
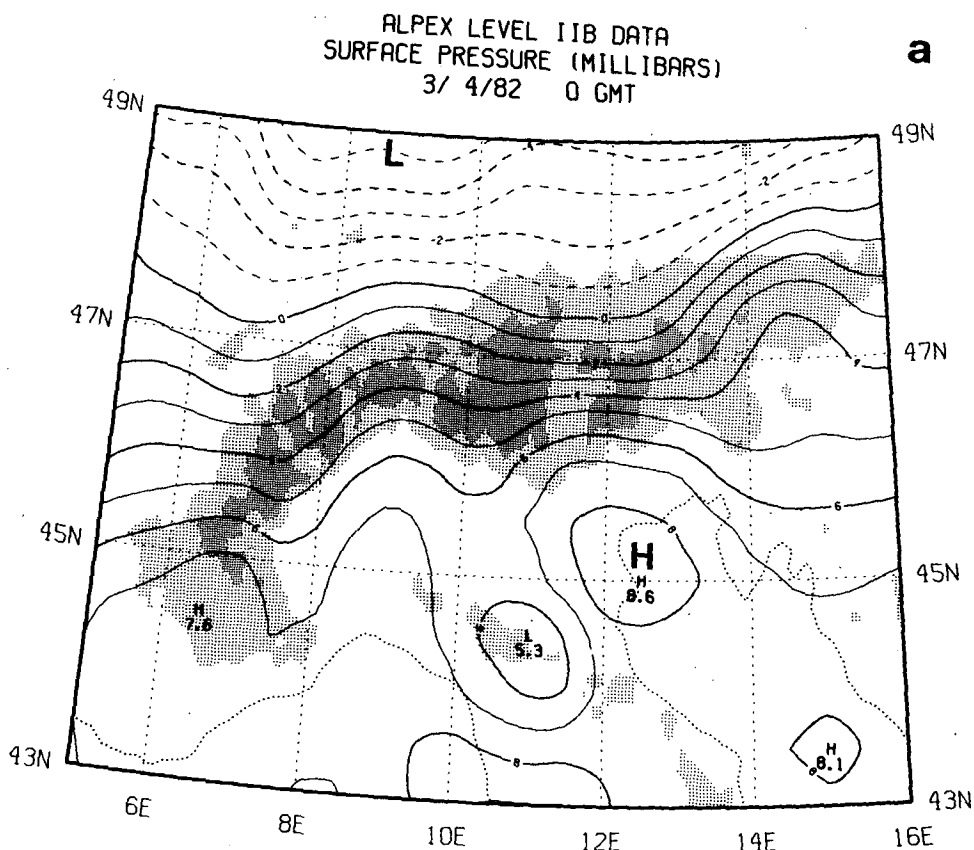
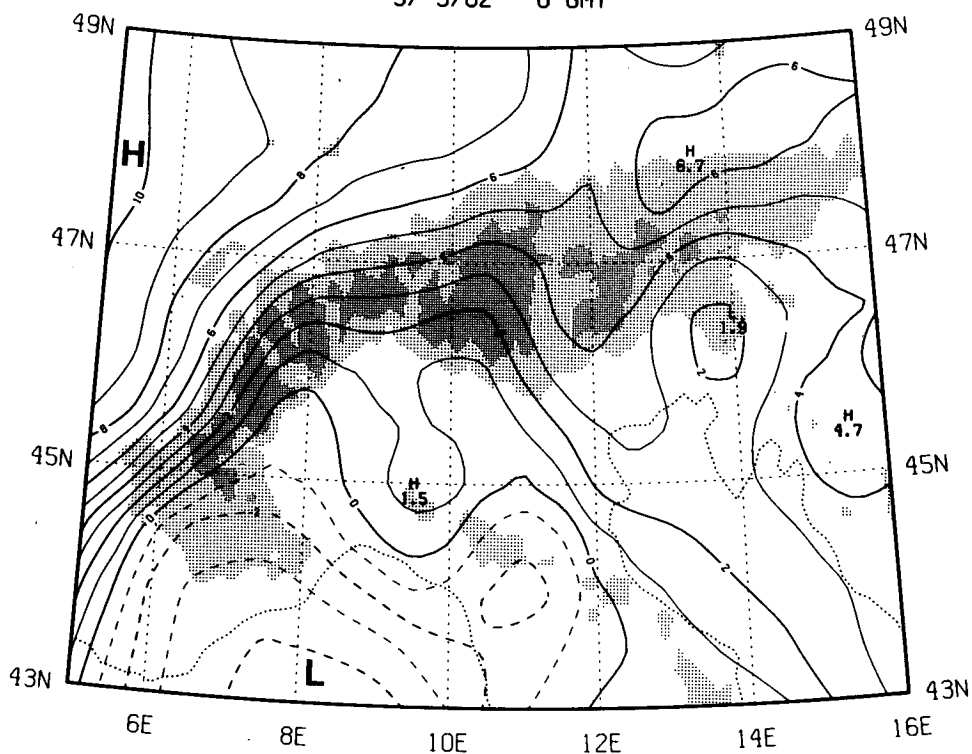


FIG. 1. Deviation surface pressure for the period of 4-5 March 1982, (a) 0000 UTC 4 March, (b) 1200 UTC 4 March and (c) 0000 UTC 5 March. Contour interval: 1 mb; negative contours are dashed; the topography above 1000 m is stippled, with higher density stippling above 2000 m; coasts-lines are dotted. In (d) the NMC analysis for 0000 UTC 5 March is shown for comparison (analysis by B. Wyman, GFDL, Princeton, contour interval is 4 mb).

ALPEX LEVEL IIB DATA
SURFACE PRESSURE (MILLIBARS)
3/ 5/82 0 GMT

c



NMC LEVEL III DATA
PRESSURE (MB)

d

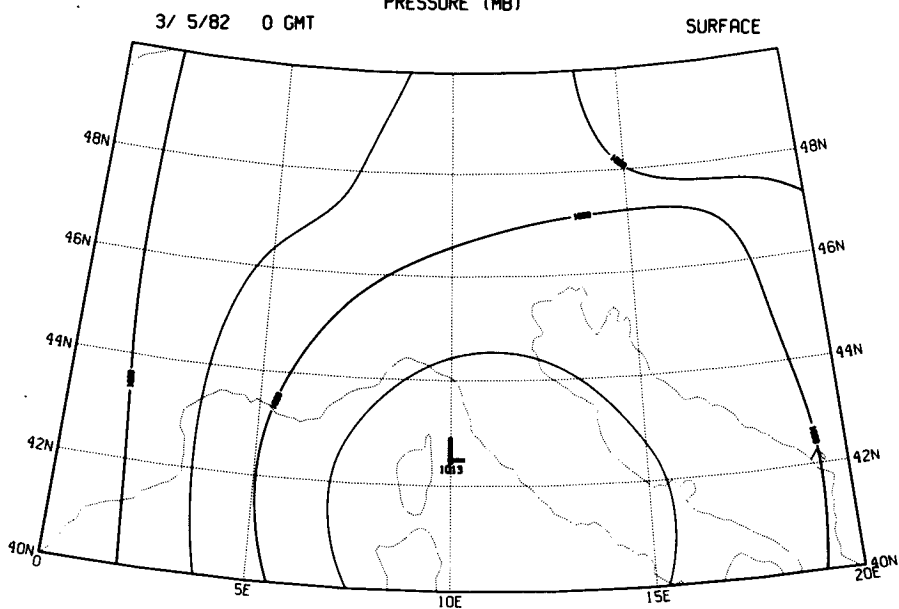


FIG. 1. (Continued)

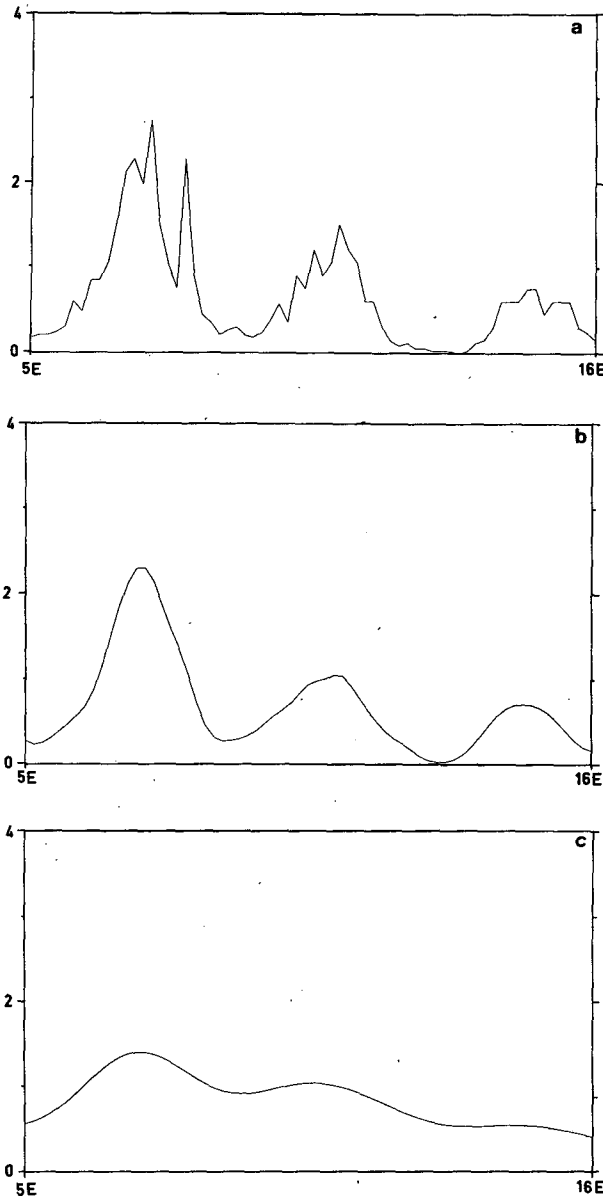


FIG. 2. Topography cross section at 46°N , from 5° to 16°E for (a) original orography, (b) resolution $R = 50$ km and (c) $R = 200$ km. The vertical domain extends from 0 to 4 km.

modulating the entire time series. A similar diurnal oscillation was also observed by Davies and Phillips (1985) for the Gotthard section and is discussed further in section 6.

The largest drag occurs on 2 March, 11 and 29 April with values close to 12.5×10^{11} N. Only slightly smaller peaks occur on 5, 16, 19 March and 9 April. These values are substantially larger than those of Hafner and Smith (1985) who reported maximum drag values of 7.7×10^{11} N on 5 March and 8.4×10^{11} N on 10 March for a mountainous region of approximately the same size, including the entire Alps. In order to com-

pare our values with those of Davies and Phillips (1985) we need an estimate of the drag per unit area. The area chosen for the comparison is crucial and, in order to be consistent, we will consider only the area of our domain which is higher than 500 m, corresponding approximately to the base level of Davies and Phillips (1985). This area is $3.0 \times 10^{11} \text{ m}^2$ (as compared with $5.9 \times 10^{11} \text{ m}^2$ for the entire domain) which leads to a drag per unit area of 4.2 Pa, compared with values as high as 7.5 Pa for the Gotthard section. If this discrepancy is real it indicates that an estimate based on the value in the Gotthard section will lead to an overestimate of the peak drag values for the entire mountain range. On the other hand, the higher values obtained in the Davies and Phillips (1985) study could be due to the higher resolution used (27 stations for 400 km). This point is discussed further in section 5.

The peak drag on the Alps is comparable in magnitude to the annual average mountain force for the latitude band 35° to 55°N estimated by Wahr and Oort (1984). A torque of 6 Hadley or $6 \times 10^{18} \text{ N m}^{-1}$ is caused by a force of approximately 12×10^{11} N at 45° latitude.

4. Composite of the strong drag events

In order to emphasize the similarities between the different strong drag events occurring during the first 20 days in March, we have constructed a composite, shown in Fig. 4, based on those cases (2, 4–5, 11, 18 March). To construct the composite we first locate the minimum drag magnitude during each of the events as our reference time and simply average the drag for a 48-h period around it.

Although the peak values are much reduced compared with some particular cases (see Fig. 3a) there is still a distinct pattern emerging from the composite. The drag reaches a first maximum in an almost northerly direction, followed by a sharp drop in magnitude (approximately 50%) and accompanied by a rapid rotation to southeasterly direction, in which the drag magnitude reaches a second maximum, slightly larger than the first. The evolution between the two maxima has taken place in approximately 18 h and follows closely the shift in wind direction from southwesterly to northwesterly associated with the arrival of the cold front.

This picture of the time evolution is in agreement with the study of Hafner and Smith (1985) and is consistent with the signature of the temporal variation of the north–south component only, in the Gotthard Pass, obtained by Davies and Phillips (1985). The strong drag values and the rapid evolution are therefore not localized in the Gotthard section.

5. Influence of resolution

In Fig. 5 we compare the drag magnitude obtained in our fine analysis ($R = 50$ km) with the drag obtained

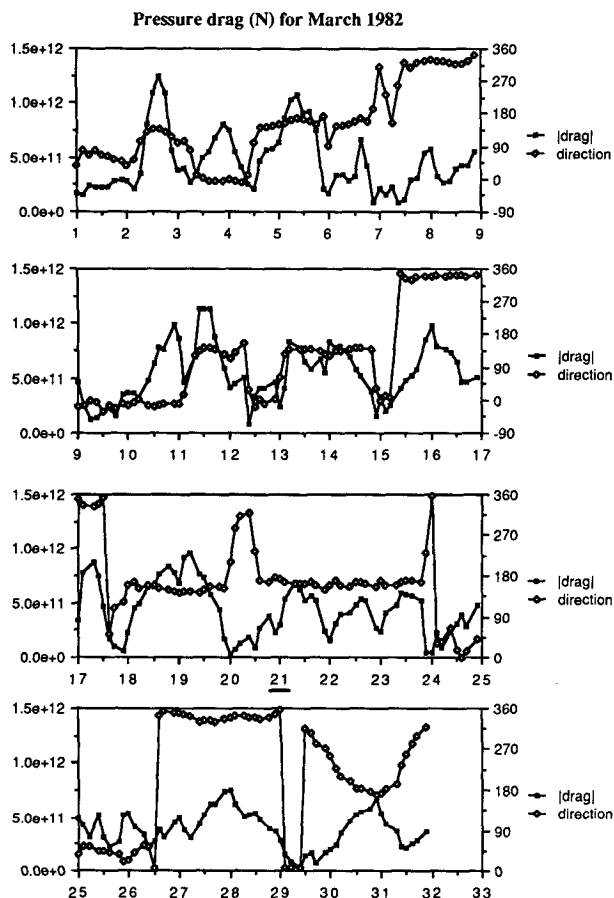


FIG. 3a. Magnitude and direction of the drag integrated over the domain shown in Fig. 1 for the month of March 1982 (resolution $R = 50$ km). Days of transition between weather periods are underlined.

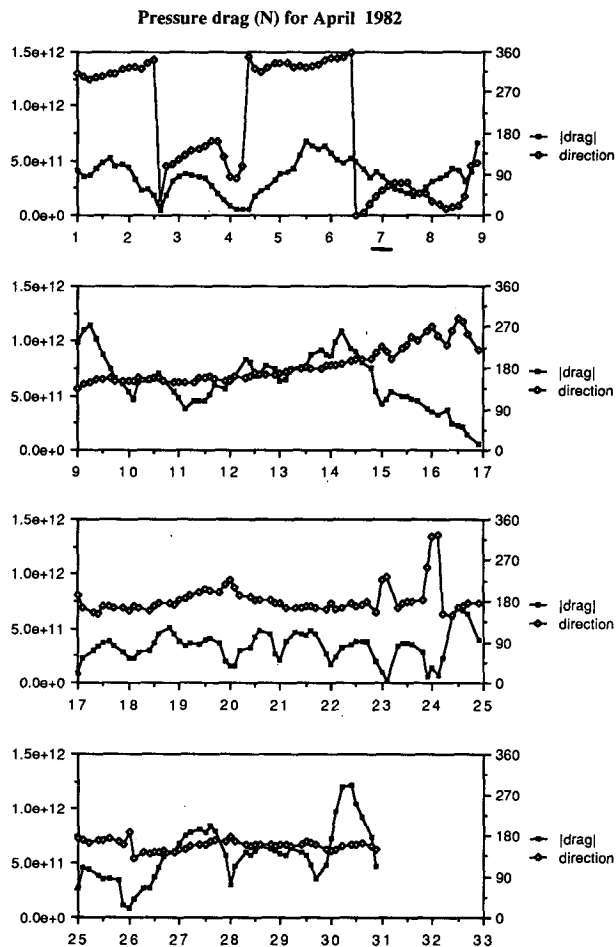


FIG. 3b. As in 3a but for the month of April 1982.

in the coarse analysis ($R = 200$ km), for the first eight days in March.

It is apparent in this figure that the strong peak values of the drag are constantly underestimated in the coarse analysis, sometimes by as much as 50%, whereas lower drag values are in better agreement. Similar results (not shown) are found for the rest of the period. The drag directions (not shown) were also compared and are in much better agreement.

The important reduction of the peak drag values due to smoothing has important implications. First, we observe that the topographic height is strongly affected by smoothing (as shown in Fig. 2), its main scale falling between 50 and 200 km. This reduction of the topographic height is not however sufficient to reduce the drag: if the pressure varies on a scale larger than the scale of the mountain and is therefore not affected by smoothing, then the drag is approximately equal to the horizontal pressure gradient multiplied by the volume of the mountain, which is conserved during the smoothing process. This implies that the drag due to a large scale (>200 km) pressure gradient will not be

sensitive to the smoothing of the topography. This in turn tells us that the peak drag values are due to pressure variations on a scale on the order of the topographic scale.

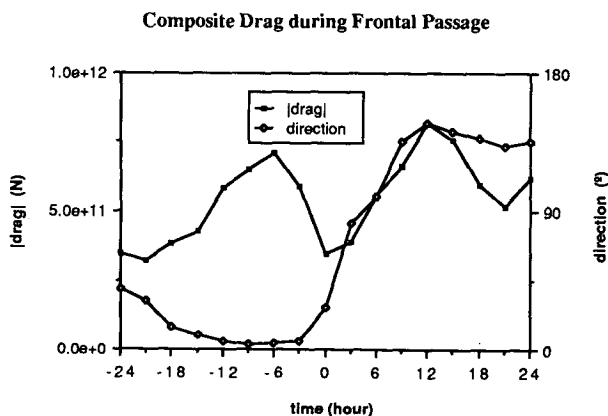


FIG. 4. Composite of the drag evolution during frontal passage.

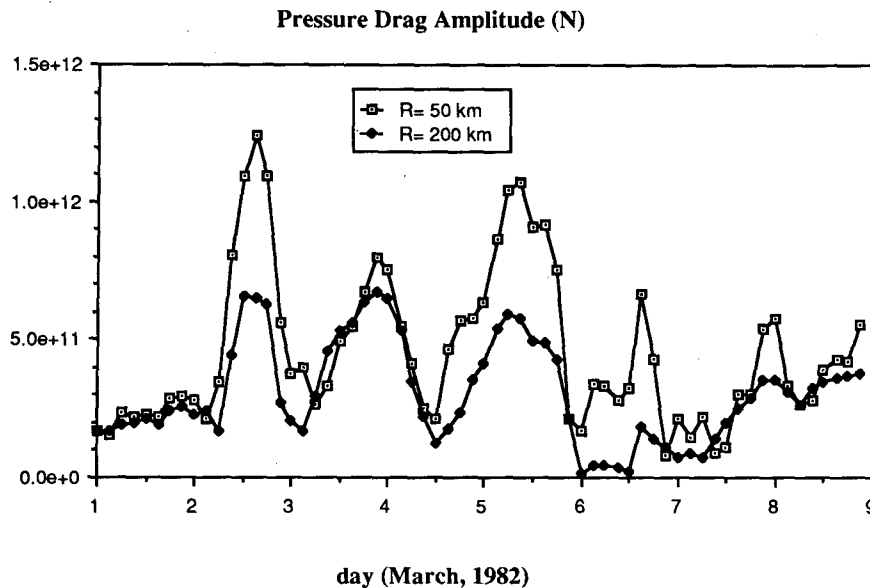


FIG. 5. Comparison of the drag magnitude obtained with different resolution for the period 1-9 March 1982.

This discussion naturally leads us to the question of what would be the drag computed with much higher resolution. In the Davies and Phillips (1985) study, the drag, computed with approximately 15 km resolution in the Gotthard pass is larger, but one can easily argue that it is not representative of the entire mountain range. Therefore, we need better data to answer this question.

6. Diurnal drag variations

A composite of the diurnal cycle for the period of 17-24 April has been constructed and is shown in Fig. 6a. As mentioned above, a similar diurnal cycle with minimum drag around 0000 UTC and maximum drag around 1500 UTC was also found in the one dimensional drag calculation of Davies and Phillips (1985) for the Gotthard section. The relative magnitude of this oscillation and the peak drag values found here are consistent with that of Davies and Phillips (1985). The additional information on the drag direction (not shown) indicates that there is no visible diurnal rotation and that the diurnal cycle is mainly in the north-south direction.

Davies and Phillips (1985) analyzed this diurnal cycle using the Hovmöller diagram of the pressure across the section as a function of time and found that the diurnal cycle in the drag is due primarily to the difference in the amplitude of the diurnal cycle of pressure on the north (~ 0.2 mb) and the south sides (> 1 mb). They argued that this difference in amplitude could be due to differences in the geometry of the valleys that compose the Gotthard pass. In Figs. 6b and 6c we see the analyzed deviation surface pressure at approximately

the time of minimum and maximum drag for 21 April, representative of the period of weak synoptic activity in April. These two figures illustrate the tendency for having (i) lower pressure to the south of the Alps compared with the north and (ii) lower pressure in late afternoon as compared with early morning. We also see by comparing Figs. 6b and 6c that the late afternoon decrease in surface pressure is more important in the south (~ 3 mb at 46°N , 9°E) than in the north (< 1 mb at 48°N , 9°E). As in the Gotthard pass drag obtained by Davies and Phillips (1985), we also see a north-south asymmetry present in the amplitude of the surface pressure diurnal cycle but here it involves the entire Alps and therefore cannot be attributed to a particular valley geometry. At present, it is not clear

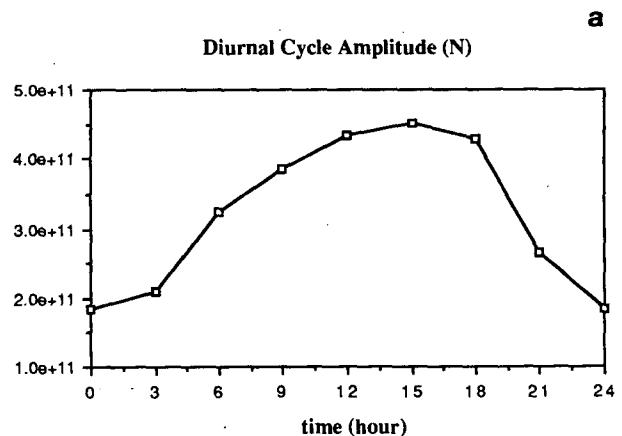


FIG. 6. (a) Average amplitude of diurnal cycle in drag magnitude for the period 17 to 24 April 1982.

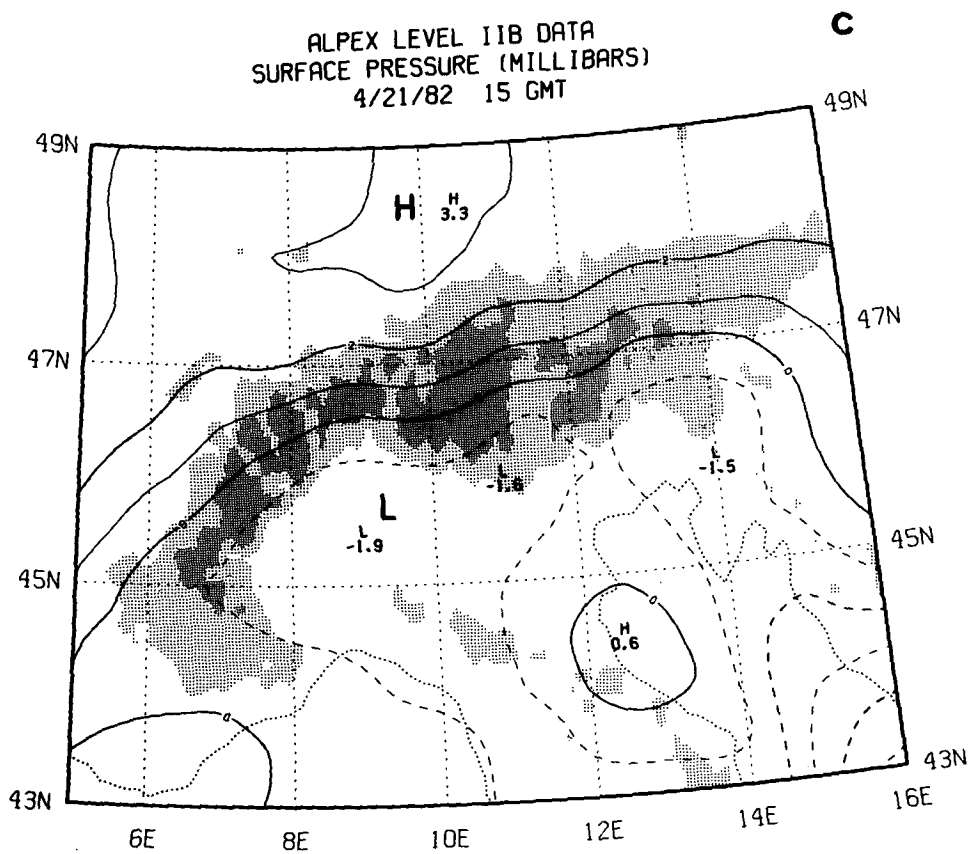
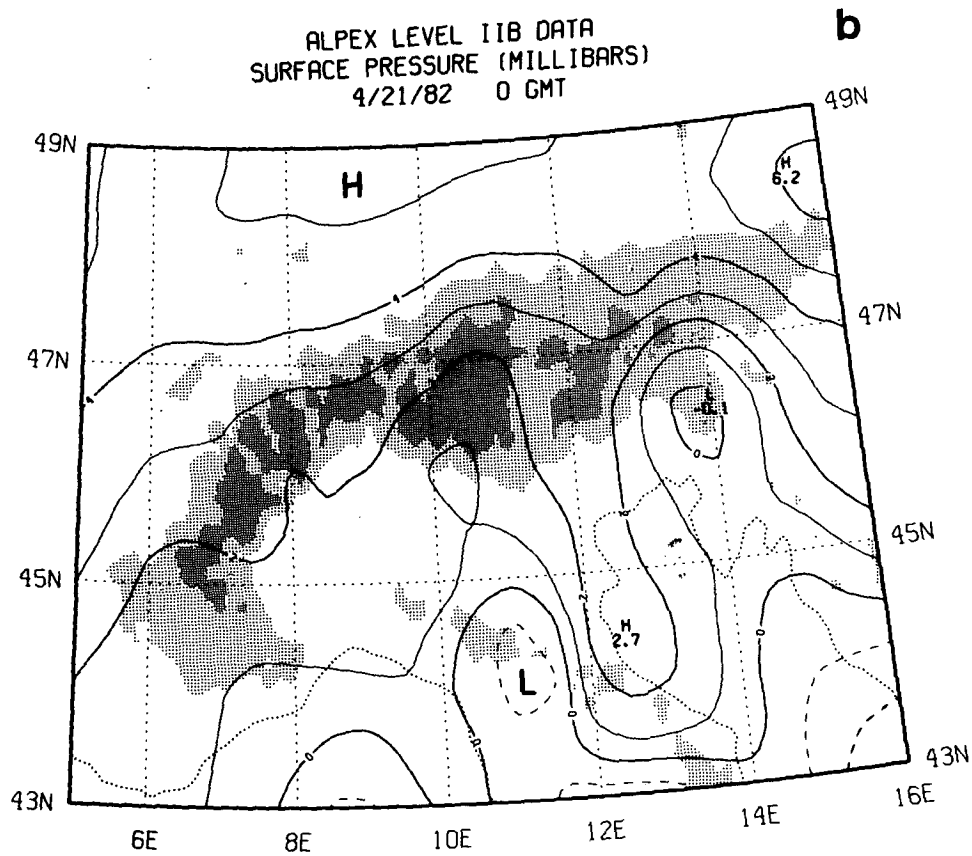


FIG. 6. (Continued) (b) and (c) Deviation surface pressure maps (contour interval: 1 mb) at the extrema of the drag diurnal cycle (0000 and 1500 UTC, respectively) for 21 April 1982. Negative contours are dashed and the orography is stippled as in Fig. 1.

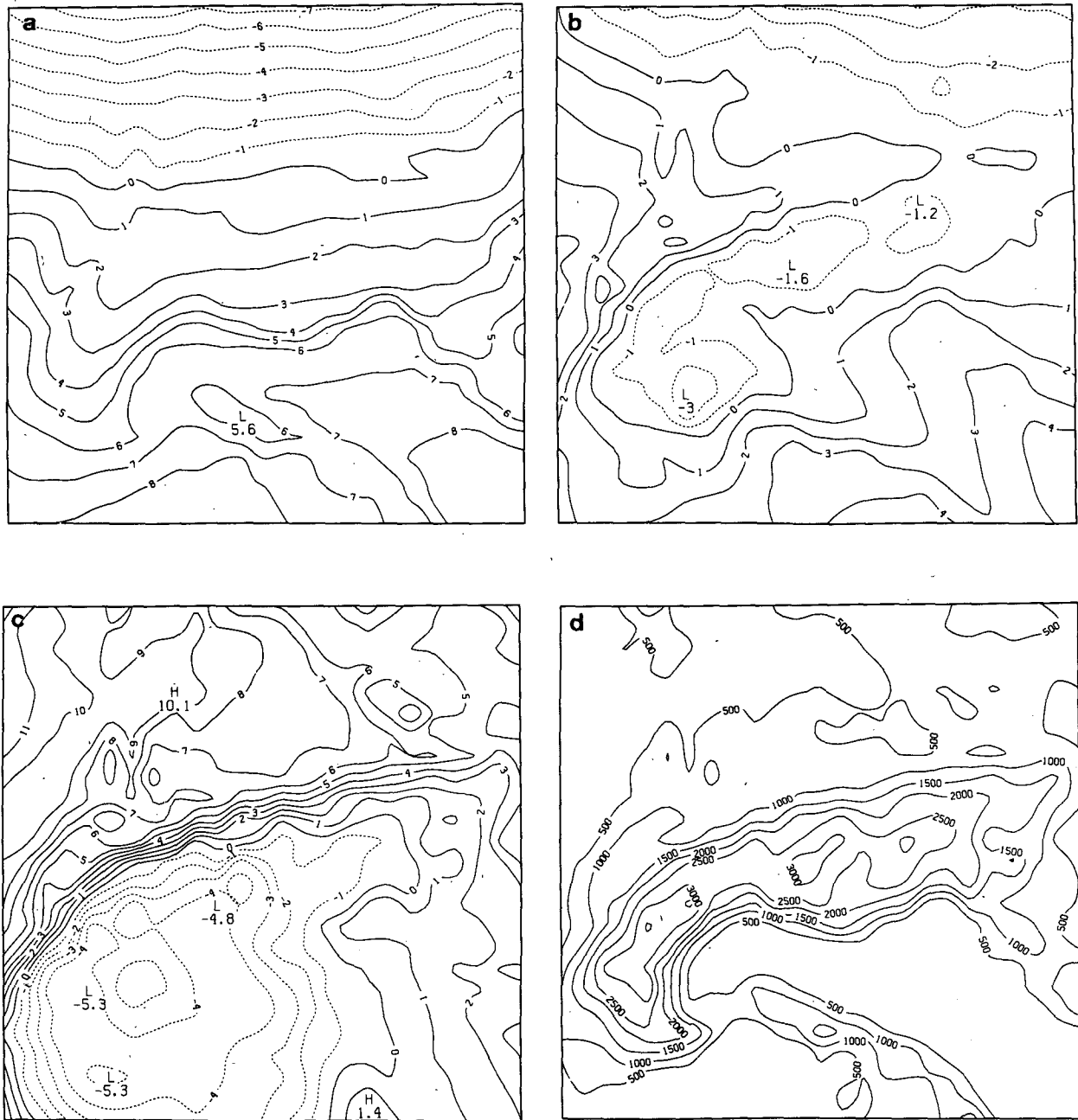


FIG. 7. Deviation surface pressure map (contour interval: 1 mb) in the numerical simulation of 4–5 March, (a) 0000 UTC 4 March, (b) 1200 UTC 4 March, and (c) 0000 UTC 5 March (compare with Fig. 1). The model topography is shown in (d).

what the exact reasons are for this asymmetry. Possible causes include the differences in the solar exposure of valleys on the north and south sides and the maritime influence of the Mediterranean Sea. Finally, we should point out that the analysis may be strongly biased toward giving strong diurnal variations because the surface pressure is more often measured in the valleys (which are subject to stronger diurnal cycle). This effect is insufficient without the asymmetry mentioned above.

7. Comparison with model drag

It was one of ALPEX original goals to use the drag computed from the array of microbarographs for comparison with drag in numerical prediction models. Such a comparison was initiated by Tibaldi and Dell'Osso (1986) for the model of the ECMWF and by using the drag computed by Davies and Phillips (1985).

In this section we present a comparison of the ob-

served drag obtained here with the drag in the numerical simulation of the cyclogenesis case of 4–5 March 1982 described in Pham (1986). The drag in the model is computed by the same method as for the observations. The 36 h simulation starts at 0000 UTC 4 March from a special analyses of the ALPEX dataset and uses the limited area model of the French Weather Bureau, with a resolution of 35 km. A similar comparison could also be easily made with any numerical model in sigma-coordinates, for which the surface pressure is a prognostic variable.

Figures 7b–d represent the deviation surface pressure at 12 h interval for a subdomain of the numerical simulation containing the Alps and are directly comparable to Figs. 1a–c. The model orography is shown in Fig. 7d. There are good similarities between modeled and observed pressure such as the tight pressure gradient located near the crest of the Alps and its reversal between 0000 UTC 4 March, and 0000 UTC 5 March, as discussed in section 3. The model results however, indicate that the pressure gradient is located on the northern slopes at 0000 UTC 5 March (Fig. 7d); but this shift is not visible in Fig. 1c and probably cannot be resolved by the analysis.

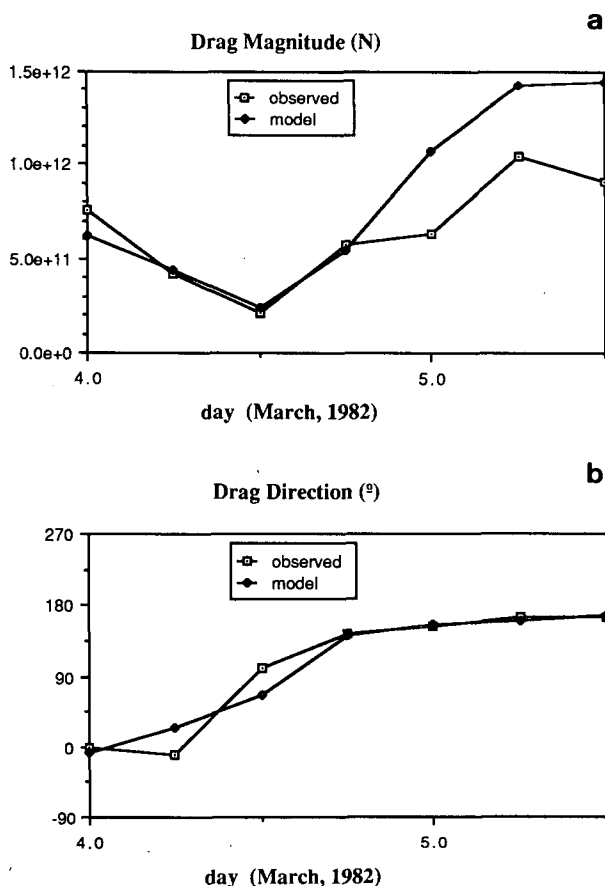


FIG. 8. Comparison of the observed drag (resolution $R = 50$ km) with the 36 h numerical simulation ($R = 35$ km), starting on 0000 UTC 4 March, (a) drag amplitude and (b) drag direction.

Figure 8 shows the comparison between model ($R = 35$ km) and observation ($R = 50$ km) for the drag magnitude and direction during the 36-h period. This is one of the strong drag events associated with frontal passage and cyclogenesis. We see that the change in drag direction from northerly to southerly is fairly well reproduced by the model and that the agreement in direction is better for stronger drag values. The observed and modeled drag magnitude are almost identical for the first 18 h of the simulation although the model drag starts slightly smaller, possibly due to initial smoothing of the pressure field. Thereafter there is an important, almost constant, overestimate of the drag by the model. Currently, we have no definitive explanation for this difference and we can only present a few hypotheses in addition to possible model shortcomings. First, the difference in resolution between the model (35 km) and the observation (50 km) might play a role (as mentioned in section 5) and be reflected in the difference in drag. In addition, the use of enhanced orography as described by Pham (1986), due to the increase of the topography volume, might also cause an artificial increase of the drag in the model similar to that reported by Tibaldi and Dell'Osso (1986). This experiment is clearly insufficient to draw firm conclusions and there is an urgent need for better comparisons to clarify these questions and also to investigate the dynamical effects of this drag on the atmosphere.

8. Summary

The mountain pressure drag has been computed using all the reported surface pressure data in a limited domain including the Alps.

The pressure analysis has been performed on a deviation surface pressure which corresponds, for each station, to the difference between the surface pressure and the standard pressure at the surface. The computed drag differs therefore from the actual drag by a constant value that represents the horizontal component of the force resulting from the weight of the atmosphere if the domain is not flat on average.

As also shown by previous studies, the drag time series is strongly correlated with the synoptic events, in particular with frontal passage and cyclogenesis. Our drag values are somewhat larger than those reported by Hafner and Smith (1985) for a mountainous domain approximately the same size but are smaller than the values of Davies and Phillips (1985) for the Gotthard section, if they are assumed to be representative for the fraction of our domain above 500 m. These discrepancies might be attributed to differences in resolution as indicated by the important decrease in peak values of the drag when the resolution is decreased. The peak drag values on the Alps are comparable, in magnitude, to the annual average mountain drag for the latitude band 35° – 55° N.

An important diurnal cycle, with minimum around

0000 UTC and maximum around 1500 UTC, is found in the magnitude of the drag during the period of weak synoptic activity in mid-April. The direction of the drag remains meridional during this cycle which is very similar to the one reported by Davies and Phillips (1985) in the Gotthard section, but involves the entire Alps.

Finally a comparison of observed drag ($R = 50$ km) with a high resolution numerical simulation ($R = 35$ km) of the 4–5 March 1982 cyclogenesis case on the Alps shows generally good agreement in the drag evolution. It shows also that the model is capable of producing the tight pressure gradients observed above the topography on 5 March.

Acknowledgments. The authors would like to thank Bram Oort and Yoshi Hayashi for helpful comments and critical review. B. Carissimo was supported during his stay at the Geophysical Fluid Dynamics Laboratory through grant NSF ATM 8218761.

REFERENCES

- Boer, G. J., N. A. McFarlane, R. Laprise, J. D. Henderson and J. P. Blanchet, 1984: The Canadian Climate Center Spectral Atmospheric General Circulation Model. *Atmos. Ocean*, **22**, 397–429.
- Batchelor, G. K., 1967: *An Introduction to Fluid Dynamics*. Cambridge University Press.
- Cox, K. W., 1986: Analysis of the Pyrenees lee wave event of 23 March 1982. *Mon. Wea. Rev.*, **114**, 1146–1166.
- Davies, H. C., and P. D. Phillips, 1985: Mountain drag along the Gotthard section during ALPEx. *J. Atmos. Sci.*, **42**, 2093–2109.
- Hafner, T., and R. B. Smith, 1985: Pressure drag on the European Alps in relation to synoptic events. *J. Atmos. Sci.*, **42**, 562–575.
- Hoinka, K., 1985: Observation of the airflow over the Alps during a foehn event. *Quart. J. Roy. Meteor. Soc.*, **111**, 199–224.
- Kuettner, J. P., 1986: The aim and conduct of ALPEx. ICSU-WMO, GARP Publ. Ser. No. 27, 3–13.
- Palmer, T. N., G. N. Shutts and R. Swinbank, 1986: Alleviation of a systematic westerly bias in general circulation and numerical weather prediction models through an orographic wave drag parameterization. *Quart. J. Roy. Meteor. Soc.*, **112**, 1001–1039.
- Pham, H. L., 1986: The role of Alpine mountain representation in lee cyclogenesis simulations. ICSU-WMO, GARP Publ. Ser. No. 27, 231–241.
- Pierrehumbert, R., 1987: An essay on the parameterization of orographic gravity wave drag. *ECMWF Seminar and Workshop on Observation, Theory and Modelling of Orographic Effects*. June, 1987, 333 pp.
- Richner, H., 1986: Analysis and quality of ALPEx data. ICSU-WMO, GARP Publ. Ser. No. 27, 31–48.
- Smith, R. B., 1982: Synoptic observations and theory of orographically disturbed wind and pressure. *J. Atmos. Sci.*, **29**, 60–70.
- Steinacker, R., 1981: Analysis of the temperature and wind field in the Alpine region. *Geophys. Astrophys. Fluid Dyn.*, **17**, 51–62.
- Tibaldi, S., and L. Dell'Osso, 1986: Representation of pressure drag effects in numerical modelling of Alpine cyclogenesis. ICSU-WMO, GARP Publ. Ser. No. 27, 207–214.
- Wahr, J. M., and A. H. Oort, 1984: Friction and mountain-torque estimates from global atmospheric data. *J. Atmos. Sci.*, **41**, 190–204.
- Wallace, J. M., S. Tibaldi and A. Simmons, 1983: Reduction of systematic forecast errors in the ECMWF model through the introduction of an envelope orography. *Quart. J. Roy. Meteor. Soc.*, **109**, 683–718.